RESEARCH PAPER

Spectroscopic Analysis, Broad-Spectrum Antimicrobial, and Phytochemical Profiling the effectiveness of the Chara zeylanica An Ecological Foundation for Upcoming Nanotherapeutics

Edison Raj Godwin P[a], Paul Ajithkumar I[a*], Dharmaraj Praveen kumar[c], A.K. Arun Prasath[b], Karthikeyan Ravichandran[e] and Daniel Jebaraj P[d]

[a]*Department of Botany , Bishop Heber College (Autonomous) Affiliated to Bharathidasan University Trichy -620017 , Tamil Nadu, India*
[b]*Centre for climate change Research (CCCR), Department of Environmental Biotechnology, Bharathidasan University, Tiruchirappalli 620024, Tamil Nadu , India*
[c]*Kirnd Bionano Pvt Ltd, No 12 Mariamman Nagar, Ayyanpudur , Trichy -620007 , Tamil Nadu , India*
[d]*Department of Chemistry, Jamal Mohamed College (Autonomous), Affiliated to Bharathidasan University, Trichy,620020, India*
[e]*Department of Physics, Jamal Mohamed College (Autonomous), Affiliated to Bharathidasan University, Trichy,620020, India*
***Corresponding Author:** paulajith@bhc.edu.in*

Received: 24th April, 2026; Revised: 20th May 2026; Accepted: 30th June, 2026; Available Online: 10th July, 2026

ABSTRACT

The growing global issue of multidrug-resistant (MDR) infections could be significantly mitigated by macroalgae, a substantial yet largely unexplored source of structurally diverse bioactive chemicals. This research investigates the complex phytochemical profile of the green macroalga Chara zeylanica, including qualitative and quantitative analyses and the dual-action pharmacological efficacy of its extracts, focusing on its broad-spectrum antioxidant and antibacterial properties. Systematic sequential solvent extraction revealed that the aqueous and ethanolic fractions had the largest concentrations of secondary metabolites, including high concentrations of alkaloids, polyphenols, flavonoids, and saponins. The extract was thoroughly examined using Ultraviolet-Visible (UV-Vis), Fourier-Transform Infrared (FTIR), and Gas Chromatography-Mass Spectrometry (GC-MS) to identify the chemical components responsible for this bioactivity. A very complex matrix containing 135 distinct secondary metabolites was effectively resolved using high-resolution GC-MS profiling. A synergistic trio of volatile compounds, branched terpenoids, and long-chain fatty acids quantitatively dominates this complex chemical library. Pharmacological analyses revealed a highly complex dual-mode treatment profile. In the DPPH antioxidant assay, the extract showed a strong, dose-dependent ability to scavenge exogenous free radicals, demonstrating its potent cytoprotective potential. Endogenously, the extract demonstrated strong, dose-dependent biocidal activity at 20 µg/mL, 40 µg/mL, and 60 µg/mL against important clinical strains, such as fungal strains (Candida albicans and Aspergillus niger), Gram-positive bacteria (Bacillus subtilis and Staphylococcus aureus), and Gram-negative bacteria (Klebsiella pneumoniae and Escherichia coli). Comparable to the effectiveness of typical commercial references. Importantly, the precise molecular mechanism of this bactericidal effect was revealed. In addition to its direct pharmacological potency, the rich polymeric hydroxyl (O–H) and carbonyl (C=O) structural footprints revealed by FTIR and the strong phenolic hyperchromic shifts detected by UV-Vis make the C. zeylanica aqueous matrix an ideal, environmentally friendly green nano-factory. These results clearly demonstrate that the extract is an excellent biological precursor for the thermodynamic capping and biogenic synthesis of stable metallic nanoparticles. This research offers a fundamental chemical and mechanistic framework for converting unprocessed macroalgal extracts into next-generation, aqueous-based nanotherapeutics that successfully evade traditional routes of microbial resistance

Keywords: Chara zeylanica, GC-MS profiling, Dual-Action Pharmacology, DPPH Antioxidant, Green Nanotechnology, Antimicrobial Activity, Staphylococcus aureus, Escherichia coli, Candida albicans.

How to cite this article: Godwin PER, Ajithkumar IP, Praveenkumar D, Prasath AK, Ravichandran K, Jebaraj P, Spectroscopic Analysis, Broad-Spectrum Antimicrobial, and Phytochemical Profiling the effectiveness of the Chara zeylanica An Ecological Foundation for Upcoming Nanotherapeutics. Int J Drug Deliv Technol. 2026;16(7):603-616. DOI: 10.25258/ijddt.16.7.64
Source of support: Nil.
Conflict of interest: None

INTRODUCTION

Multidrug-resistant (MDR) bacterial infections, especially aggressive Gram-negative forms such as *Escherichia coli*, are among the most serious and rapidly spreading public health emergencies of the twenty-first century (Elmaidomy *et al.,* 2022). Bacterial populations have rapidly evolved

**Author for Correspondence: paulajith@bhc.edu.in*

complex resistance mechanisms due to the widespread misuse of traditional, single-target antibiotics. The development of highly impenetrable cellular biofilms, the enzymatic degradation of antimicrobial drugs, and the overexpression of drug efflux pumps are examples of these responses (Elmaidomy *et al.,* 2022). An urgent pharmacological paradigm shift is required to investigate biogenic compounds, which naturally have multi-component chemical structures that are much less likely to induce bacterial resistance, to overcome these strong evolutionary defenses (Jo *et al.*, 2024). In this regard, macroalgae, particularly those belonging to the family Characeae, have traditionally shown great promise as long-term sources of innovative, broad-spectrum medicinal substances (Ali *et al.,* 2024).

Chara zeylanica is a common macroscopic freshwater green alga of medicinal interest because of its wide range of secondary metabolites and potent innate antibacterial activity against human pathogens. Although its macroscopic antibacterial characteristics have been noted in early baseline screens, its high-resolution mechanistic, antioxidant, and nanobiotechnological characterization of the aqueous extract has not been thoroughly investigated. The complex organic matrices in medicinal extracts must be resolved using sophisticated phytochemical profiling techniques such as UV-Vis spectroscopy, Fourier Transform Infrared (FTIR) spectroscopy, and Gas Chromatography-Mass Spectrometry (GC-MS) (Sehim *et al.*, 2023). In this study, a thorough GC-MS analysis of the *C. zeylanica* extract successfully mapped a library of 135 distinct bioactive components that were previously unidentified in terms of complexity. The primary constituents of this structural matrix are flavonoids, polyphenols, strong long-chain fatty acids, and medicinal terpenoids.

The combination of these 135 distinct functional components dictates a very intricate dual-action pharmaceutical strategy that simultaneously addresses oxidative damage and microbial multiplication. Exogenous Free Radical Scavenging The extract has remarkable antioxidant activity due to its high polyphenol and flavonoid contents. In the 2,2-diphenyl-1-picrylhydrazyl (DPPH) radical-scavenging assay, the extract exhibits an impressive, dose-dependent ability to neutralize the free radicals. These biogenic compounds easily donate electrons or hydrogen atoms to stabilize reactive species through Hydrogen Atom Transfer (HAT) and Single Electron Transfer (SET) mechanisms; they may be a powerful cytoprotective agent against systemic oxidative stress (Tako *et al.,* 2020).

Substantial presence of electron donating functional groups, such as polymeric hydroxyl (-OH) and carbonyl (C=O) groups, is revealed by FTIR-based biochemical characterization of the *C. zeylanica* extract. Green nanobiotechnology extensively uses these organic stabilizing and capping compounds (Ali *et al.*, 2024). The macroalga is a perfect, environmentally acceptable precursor for the green synthesis of biogenic nanoparticles and for stand-alone treatment because of its inherent thermodynamic capacity to reduce metallic precursor ions and stabilize the resulting nanostructures.

This study attempts to establish the *Chara zeylanica* aqueous extract as a leading, sustainable platform by combining thorough chemical profiling (UV, FTIR, GC-MS) with dual-faceted pharmacological mapping that includes both potent extracellular radical scavenging (DPPH assay) For the development of targeted, next-generation nanotherapeutics to successfully address the MDR problem in clinical pathogens, its ideal biochemical design holds great potential.

2. MATERIALS AND METHODS

2.1. Macroalgal Biomass Collection and Processing

In the lotic habitat of the Vellar River in the Pudukkottai region of Tamil Nadu, India, fresh biomass of the macroscopic green alga *Chara zeylanica* routinely collected. In order to remove adhering ecological detritus, epiphytes, and sand particles, the collected macroscopic specimens were first thoroughly washed with local river water. Then followed by a tertiary rinsing with sterile distilled water. To stop thermolabile secondary metabolites from degrading, the virgin biomass was shade dried for 15 days under ambient, controlled laboratory settings (25 ± 2°C). Before sequential extraction, the algal material was mechanically ground into a fine, uniform powder using a sterile mechanical blender and kept at 4°C in an airtight desiccator.

2.2. Solvent Extraction with Polarity Guidance

A polarity guided sequential solvent extraction paradigm is used to extract bioactive phytoconstituents. sequence of solvents with increasing polarity chloroform, acetone, ethanol, methanol, and aqueous menstruum were used to sequentially extract 50 g of the ground *C. zeylanica* biomass. To guarantee maximum metabolite recovery, the extraction cycle for each solvent was maintained for a full day at its respective boiling points. The resulting crude extracts were then lyophilised after being filtered through Whatman No. 1 filter paper and concentrated in vacuo using a rotary evaporator under low pressure. The dried crude extracts were cryopreserved at -20°C for subsequent bioassays after being measured for percentage yield.

2.3. Qualitative and Quantitative Profiling of Phytochemicals

In order to identify the presence of essential phytoconstituents such as alkaloids, flavonoids, phenols, tannins, saponins, and quinones, the concentrated extracts were first put through a thorough qualitative phytochemical screening using standardised analytical techniques..

2.4. Advanced Instrumental Characterization

A combination of spectroscopic and chromatographic techniques was used to accurately determine the molecular architecture of the most active extract. A double-beam UV-Vis spectrophotometer was used to optically scan the aqueous extract between 200 and 800 nm. This described

the transitional heteroatoms and conjugated pi-electron systems that are inherent in the algal metabolites. Fourier-Transform Infrared (FTIR) spectroscopy was used to characterise the functional group. By analysing the extract in the mid-infrared transmittance range of 4000–400 cm^{-1}, particular vibrational frequencies that corresponded to functional moieties were identified. Gas Chromatography-Mass Spectrometry (GC-MS) was used to structurally uncover the volatile and semi-volatile biomolecular composition. Using a high resolution capillary column and a mass detector, chromatographic separation was accomplished. In order to identify the 135 GC-MS peaks, their mass spectra and retention periods were compared with those found in the NIST and Wiley mass spectral databases. Additionally, comparisons with Adams (2017) for volatile components were made. Calculating the primary active ingredients' relative abundance.

2.5. *In Vitro* Antimicrobial Efficacy Assay

The antimicrobial potential of *C. zeylanica* extract was assessed using Gram-negative bacteria (*Klebsiella pneumoniae and Escherichia coli*), Gram-positive bacteria (*Bacillus subtilis and Staphylococcus aureus*), and fungal strains (*Candida albicans and Aspergillus niger*) using the standardized agar well diffusion method. Herein, the Microbial inocula were adjusted to 0.5 McFarland standard turbidity and swabbed uniformly onto Mueller-Hinton Agar (MHA) for bacterial strains and Sabouraud Dextrose Agar (SDA) for fungal strains. Further, a well size of 6 mm diameter was bored, and the extract with various dosages, namely 20, 40, and 60 µg/mL, was inoculated. Streptomycin is used as a positive control for bacterial strains, and fluconazole is used as a control for fungal strains. Following 24 h incubation for bacteria at 37 °C and 48 h incubation for fungi at 28 °C, the zone of inhibition (ZOI) in mm is measured.

2.6 In Vitro Antioxidant Activity

The *Chara zeylanica* aqueous extract's free radical scavenging capacity was quantitatively evaluated using the standard 2,2-diphenyl-1-picrylhydrazyl (DPPH) colorimetric micro-assay. The antioxidant phytoconstituents in the extract transform the stable, deep-violet DPPH radical into a non-radical, pale-yellow derivative, diphenylpicrylhydrazine, via Single Electron Transfer (SET) and Hydrogen Atom Transfer (HAT). The fundamental methodology (Brand-Williams *et al.*, 1995) served as the basis for the test protocol, which was modified somewhat for the purpose of assessing macroalgal aqueous matrices (Sáez-González *et al.,* 2024). Commercial sources provided all analytical-grade reagents, including high-purity methanol and DPPH reagent. The positive pharmacological reference standard was rutin, a well-known and potent flavonoid.

3. RESULTS AND DISCUSSION

Numerous secondary metabolites are produced by aquatic macroalgae as defense mechanisms against biotic and abiotic environmental stressors. To evaluate the differential solubility and partitioning of active phytoconstituents, *Chara zeylanica* was subjected to a preliminary qualitative phytochemical screening over a solvent gradient of methanol, ethanol, acetone, chloroform, and water. Alkaloids, sugars, phenols, triterpenoids, saponins, and flavonoids were among the secondary metabolites identified in the study their quantities varied significantly with solvent polarity (Table 1). Alkaloids, phenols, and saponins were abundant in the aqueous extract, which had the highest extraction efficiency. The acetone, methanol, ethanol, and chloroform extracts had a modest degree of component diversity. Crucially, the broad-spectrum antibacterial activity found is substantially correlated with the amount of phenols and alkaloids in the ethanolic extract. These functional groups are known to interact with microbial DNA and disrupt bacterial cell membrane integrity (Cowan, 1999).

Table 1. Qualitative phytochemical screening of *Chara zeylanica* extracts across varying solvent polarities.

Phytoconstituent	Methanol	Ethanol	Acetone	Chloroform	Aqueous
Alkaloids	+++	+	++	++	++
Carbohydrates	++	-	-	-	++
Proteins	-	+	-	-	+
Phenols	+++	+++	++	+	+
Triterpenoids	-	-	+++	-	+
Saponins	++	+++	-	-	+
Steroids	-	+	-	-	-
Amino Acids	-	+	-	-	+
Tannins	+	+	-	+	+
Flavonoids	+	+	-	-	++
(Key: +++ = highly present, ++ = moderately present, + = weakly present, - = absent)					

Quantitative assessment of phytochemicals. The first screening has been quantitatively validated by calculating the secondary metabolite profile. In modern pharmacognosy, secondary metabolites from plants and algae are highly valuable as primary molecular scaffolds in drug development (Edreva *et al.,* 2008).Total Phenolic Content (TPC) Phenolic chemicals are powerful cellular antioxidants and direct antibacterial agents. The results of the quantitative study showed that the methanolic extract had the highest TPC (1.035 mg GAE/g), followed by the acetone extract (0.08 mg GAE/g), ethanol extract (0.546 mg GAE/g), and chloroform extract (0.428 mg GAE/g).

The enrichment of phenolics in highly polar solvents can account for the higher bioactivity found in the methanolic fractions. The TFC uniformly distributed throughout the extracts, peaking in the aqueous (1.213 mg GAE/g) and chloroform (1.247 mg GAE/g) fractions, then in the acetone (1.121 mg GAE/g) and methanol (1.119 mg GAE/g) fractions. The pharmacological potential of total alkaloid and tannin content, to inhibit enzymatic pathways and microbial growth has been well established in contemporary medicine. The quantitative analysis found that the methanolic extract (1.099 mg GAE/g) and the chloroform extract (1.208 mg GAE/g) had the highest concentrations of both tannins and alkaloids.

Gas Chromatography-Mass Spectrometry (GC-MS) was used to molecularly characterize the volatile and semi-volatile composition of the ethanolic extract, despite its enhanced phytochemical yield and downstream antibacterial activity. 135 distinct bioactive compounds were identified by the chromatogram's retention durations (Rt), molecular formulas, and relative percentage peak areas (Table 2). The chromatogram revealed 135 distinct bioactive compounds based on their relative peak area percentages, molecular formulas, and retention times (Rt) (Table 2). Gas Chromatography-Mass Spectrometry (GC-MS) was used to fully analyze the metabolomic profile of the Chara zeylanica extract, revealing an incredibly rich chemical variety consisting of 135 secondary metabolites (Table 2). Volatile, semi-volatile, non-polar lipophilic, and polar derivatized compounds are clearly separated in the total ion chromatogram (Figure 1) throughout a retention time (Rt) range of 3.25 to 29.99 minutes

Table 1. GC-MS molecular profiling of the bioactive Ethanolic extract of *Chara zeylanica*.

Peak#	RT	Name	Area	Area %
1	3.25	Propane, 1,1-diethoxy-	23623	0.10
2	3.79	PROPANE, 1-(1-ETHOXYETHOXY)-	21131	0.09
3	3.85	Propane, 1-(1-ethoxyethoxy)-	19424	0.08
4	4.02	Acetic acid, chloro-	11164	0.05
5	4.13	trans-dideuterioxy-cyclopentene	16030	0.07
6	4.21	(3-ethynyl-3-methyloxiran-2-yl)methanol	7575	0.03
7	4.35	1-phenyl-5-(.alpha.,.beta.-dibromophenethyl)-1h-tetrazole	41249	0.18
8	4.65	Cyclopropane, 1,1-difluoro-2,3-dimethyl-, trans-	42030	0.18
9	4.79	Triethylsilanol	89222	0.39
10	5.12	2-mercaptothiazole	45208	0.20
11	5.33	4-amino-1,2,5-oxadiazol-3-ol	9295	0.04
12	5.49	2-hydroxy-3-methylbutanoic acid	3245871	3.05
13	5.63	Octane, 4-bromo-	241839	1.05
14	5.95	5-nonanol, 5-methyl-	126066	0.55
15	6.71	3-hydroxy-4,4- dimethyldihydrofuran-2(3H)-one	154033	0.67
16	6.97	4-Piperidinamine, N,1-dimethyl	3616474	4.07
17	7.72	Acetamide, n-ethyl-	71756	0.31
18	8.24	Cyclohexan-1,4,5-triol-3-one-1-carboxylic acid	22132	0.10
19	9.05	1-heptanol, 2,4-dimethyl-,	76016	0.33
20	9.20	4h-pyran-4-one, 2,3-dihydro-3,5-dihydroxy-6-methyl-	674935	1.94
21	9.25	3-hepten-2-ol, (z)-	94593	1.59
22	9.27	Methoxyacetic acid, octyl ester	21641	0.94
23	9.32	Ethanamine, 2-(methylthio)-	9797	0.04
24	9.35	1H-pyrazol-4-ylmethanamine	25136	0.11
25	9.41	Acetic acid, nonyl ester	60584	0.26
26	9.47	2-methoxy, 4-vinylphenol	18047	0.08
27	9.51	2-(acetyloxy)-1-carboxyethanaminium chloride	11414	0.05
28	9.55	3-Phenylpropanol, tms derivative	207848	0.91
29	9.67	3,5-dimethyl cyclopentenolone	191962	0.84
30	9.69	2-acetylcyclopentanone	54350	0.24
31	9.71	1,3-cyclopentanedione, 2,4-dimethyl-	139218	0.61
32	9.72	o-cresol	62768	0.27
33	9.75	1,2-Benzenedicarboxylic acid	4439325	2.72
34	10.46	2,4,6-trimethyldecane	85277	0.37
35	11.32	9-(4-hydroxyphenyl)-3,3,6,6-tetramethyl-3,4,6,7,8a,9-hexah	238642	0.04
36	11.69	10-undecen-1-ylester	7661711	1.03
37	11.72	Heptanal	107990	0.47
38	11.75	2-heptenoic acid	48220	0.21
39	11.83	Methoxyacetic acid, nonyl ester	72725	0.32

40	11.89	Acetic acid, 2,2'-[oxybis(2,1-ethanediyloxy)]bis-	134659	0.59
41	11.94	2-methoxy-4-vinylphenol	758302	3.30
42	12.05	Dimethylamine, tms derivative	105585	0.46
43	12.18	1,3-cyclohexanediol	339061	1.48
44	12.45	1,3-oxathiolan-5-one, 2-(1,1-dimethylethyl)-4-(1-hydroxy-2	254472	1.11
45	12.77	cis-2-ethylcyclopentanecarboxaldehyde	129971	0.57
46	12.84	1,2,5-trimethyl-4-piperidinone thiosemicarbazone	1544061	2.67
47	12.89	1h-azonine, octahydro-1-nitroso-	69527	0.30
48	12.92	5-o-methyl-d-gluconic acid dimethylamide	172031	0.75
49	13.16	1r,3-trans-dimethoxy-2-methylcyclohexane	51461	0.22
50	13.37	Butyric acid, 4-(3,5-dimethylpyrazol-1-yl)-4-oxo-	9106	0.04
51	13.52	Caryophyllene	3876233	1.01
52	13.66	Cyclopentane, 1,3-dimethoxy-, trans-	319076	0.39
53	13.71	Chlorozotocin	215952	0.94
54	13.75	Carbonic acid, but-3-yn-1-yl nonyl ester	73475	0.32
55	13.84	Ethyl 2-methyl-1-propenylsulfide #	87245	0.38
56	14.36	.beta.-d-glucopyranose, 1,6-anhydro-	136285	0.59
57	14.59	4-methyl-1,2,5-oxadiazole-3-carboxylic acid	60321	0.26
58	14.79	Benzene, fluoro-	135428	0.59
59	14.93	4-thiazolidinecarboxylic acid, 5,5-dimethyl-	9219	0.04
60	15.15	Tetradecanoic acid	538072	1.23
61	15.25	1-(4-hydroxy-6-hydroxymethyl-tetrahydro-pyran-2-yl)-1	42606	0.19
62	15.46	1,2,3,4-cyclohexanetetrol	45896	0.20
63	15.62	Nonanoic acid, cyclohexylmethyl ester	48391	0.21
64	15.69	3-methyl-3-[(2-oxopropyl)amino]-2-butanone #	47752	0.21
65	15.72	Propanoic acid, 2-methyl-, 2-ethyl-3-hydroxyhexyl ester	15612	0.07
66	15.89	2-oxazolamine, 4,5-dihydro-5-(phenoxymethyl)-n-[(phenylamino)carbonyl]-	123466	0.54
67	16.07	Palmitic acid	6703225	1.29
68	16.22	1,3,4,5-tetrahydroxy-cyclohexanecarboxylic acid	5498778	0.94
69	16.58	5(4h)-indanone, 3a,7a-dihydro-7a-methyl-, trans-	315665	1.37
70	16.64	1,3-cyclohexanediol, 4,6-dimethyl-2-nitro-, monoacetate	303750	1.32
71	16.71	4-piperidinamine, n,1-dimethyl-	595076	2.59
72	16.95	16-methoxy-14-oxohexadec-15-enoic acid, methyl ester	309463	1.35
73	17.02	n-Hexadecanoic acid	362119	1.58
74	17.16	1,2,3,4-cyclopentanetetrol, (1.alpha.,2.beta.,3.beta.,4.alpha.)-	544505	2.37
75	17.58	1-methyl-4-(2-methyl-2-oxiranyl)-7-oxabicyclo[4.1.0]hepta	483213	2.10
76	17.61	Oleic acid	171815	0.75
77	17.69	2-nonenal	129271	1.56
78	17.78	Cyclohexane, 1,4-dimethoxy-2-methyl-, stereoisomer	96123	0.42
79	17.91	3-hepten-2-one, 4-methyl-	37634	0.16
80	18.56	2(4h)-benzofuranone, 5,6,7,7a-tetrahydro-6-hydroxy-4,4,7a	513752	2.24
81	19.62	9-octadecenal, (z)-	4889921	2.13
82	20.48	Hexadecanoic acid	459021	0.20
83	20.79	Neophytadiene	557322	2.43
84	21.06	3,7,11,15-tetramethyl-2-hexadecen-1-ol	8485032	2.37
85	21.15	3,7,11,15-tetramethyl-2-hexadecen-1-ol	1839122	0.80
86	21.39	3,5-octadienoic acid, 7-hydroxy-2-methyl-, [r*,r*-(e,e)]-	30252	0.13
87	21.55	n,n-dimethyl-1-nonadecanamine #	67778	0.30
88	22.63	2-(2-diethylaminoethylamino)ethanol	109461	0.48
89	23.38	Linolenic acid	13359	0.06
90	23.76	9-octadecenoic acid (z)-	15580525	10.68
91	23.81	Benzoic acid, 2-(1-oxopropyl)-	2113371	0.92
92	23.85	6-ethoxy-6h-[1,2]oxazine-6-carbonitrile	716562	0.31
93	23.92	Hexadecanoic acid, ethylester	1973952	0.86
94	24.06	1-(methyleneamino)-4-acetylbenzene	285031	0.12
95	24.11	Limonen-6-ol, pivalate	223193	0.10

96	24.29	1,2-butanediol, 1-(2-furyl)-	24250	0.11
97	24.32	Strearic acid	364585	1.16
98	24.35	succinic acid, tridec-2-yn-1-yl 1-phenylpropyl ester	53825	0.23
99	24.44	cis-4-methyl-exo-tricyclo[5.2.1.0(2.6)]decane	66188	0.29
100	24.61	3-hexin, 2,2-dimethyl-1-dimethylamino-	225095	0.98
101	24.65	trans-1,4-cyclohexanedimethanol, bis(pentafluoropropionate)	112316	0.49
102	24.69	6-ethoxy-6h-[1,2]oxazine-6-carbonitrile	10325	0.04
103	24.72	2h-thiopyran, tetrahydro-2-methyl-3-propyl-	10096	0.04
104	24.84	Exo-norborneol, pentafluoropropionate	12373	0.05
105	24.91	Phytol	12525	0.45
106	24.97	Hexadecanoic acid, ethyl ester	45323	0.20
107	25.12	Octadecanoic acid	3226	0.01
108	25.32	Methylmethylenimine (n-b) (e)-2-cyclohexylvinyl-bis(trifluoromethyl)borane	5207	0.02
109	25.44	3,7,11,15-Tetramethyl-2-hexadecen-1-ol	41039	0.18
110	25.51	Carbonic acid, 2-dimethylaminoethyl neopentyl ester	129431	0.56
111	25.57	Cyclohexanecarboxylic acid, heptyl ester	22411	0.10
112	25.68	1-methoxymethyl-3-(3'-methylenecyclopentyl)cyclopen	6063	0.03
113	25.72	(1sr,1'rs,2'rs)-1-(2-vinylcyclobutyl)ethanol	4435	0.02
114	25.79	2-pentanone, 4-cyclohexylidene-3,3-diethyl-	4355	0.02
115	25.82	Spiro[2.4]heptane-5-methanol, 5-hydroxy-	26974	0.12
116	25.95	2-furanmethanol	6041	0.03
117	26.01	4(1h)-pyrimidinone, 5-methoxy-	61454	0.27
118	26.25	Palmitaldehyde, diallyl acetal	37588	0.16
119	26.31	3-Eicosene	122893	0.54
120	26.49	4-chloro-3-methyl-3-methoxybutanoic acid,methyl ester	13328	0.06
121	26.53	9,12-octadecadienoic acid (z,z)-, 2-[(trimethylsilyl)oxy]-1-	2011	0.01
122	26.73	1-(2-fluoro-5-methyl-4-nitrophenyl)-4-methylpiperazine #	18362	0.08
123	26.95	2-amino-4-hydroxylaminopyrimidine	2618	0.01
124	27.36	cis-9-eicosenoic acid	8407	0.04
125	27.51	Docosanoic acid	48661	0.21
126	27.85	Tetracosane	83290	0.36
127	27.96	6,8-dioxabicyclo[3.2.1]octan-4-one, oxime	25888	0.11
128	28.06	Chloroacetic acid, undecyl ester	48354	0.21
129	28.15	9,12,15-octadecatrienoic acid, 2-[(trimethylsilyl)oxy]-1-[[(	3226	0.01
130	28.46	1,3-naphthalenediol, decahydro-, (1.alpha.,3.alpha.,4a.alp	20671	0.09
131	29.52	Stigmasterol	3003632	2.31
132	29.86	β-Sitosterol	1014591	2.44
133	29.95	Cholestan-3-one, cyclic 1,2-ethanediyl acetal (5á)-	30296	0.13
134	29.97	4-thiazolin-2-imine,3-(2-cyclohexenylethyl)-2-(4-methoxyphenyl)-4-phenyl-	11337	0.05
135	29.99	9-nonylphenyl-3,6,9-trioxanonanol, mix of isomers	25028	0.11

Despite the improved phytochemical yield and downstream antibacterial activity of the ethanolic extract, Gas Chromatography-Mass Spectrometry (GC-MS) was used to molecularly map its volatile and semi-volatile architecture. The chromatogram resolved 135 different bioactive chemicals, which were identified by their retention durations (R_t), molecular formulae, and relative percentage peak areas (Table 2) Gas Chromatography-Mass Spectrometry (GC-MS) was used to extensively analyse the metabolomic profile of the *Chara zeylanica* extract, and the results showed an incredibly rich chemical diversity consisting of 135 distinct secondary metabolites (Table 2). Over a retention time (R_t) range of 3.25 to 29.99 minutes, volatile, semi-volatile, non-polar lipophilic, and polar derivatized compounds are clearly separated in the total ion chromatogram (Figure 1). A few major peaks establish the extract's quantitative dominance these peaks combine with smaller components to produce broad-spectrum biological action. Four major classes of Long Chain Fatty Acids and Esters make up the extract's primary chemical architecture. The most prevalent single component is 9-octadecenoic acid (Z)- (Oleic acid) (Peak 90, R_t = 23.76 min, 10.68%), followed by n-Hexadecanoic acid (Palmitic acid) (Peak 73, R_t = 17.02 min, 1.58%; Peak 60, R_t = 15.15 min, 1.2), and fatty aldehydes like 9-octadecenal (z)- (Peak 81, R_t = 19.62 min, 2.13%). Nitrogenous and Heterocyclic Amines, which is a major nitrogen-containing fraction, was identified as 4-Piperidinamine, N,1-dimethyl (Peak 16, R_t = 6.97 min, 4.07% and Peak 71, R_t = 16.71 min, 2.59%), along with

1,2,5-trimethyl-4-piperidinone thiosemicarbazone (Peak 46, R_t = 12.84 min, 2.67%). These basic nitrogen moieties produce highly localised alkaline/nucleophilic conditions that can interact with biomembranes. The primary phenolic monomer is identified as 2-methoxy-4-vinylphenol (Peak 41,R_t= 11.94 min, 3.30%), a critical low molecular weight aromatic molecule with highly reactive vinyl and methoxy functional groups. Terpenoids and Phytosterols is an isoprenoid pathway that produced important bioactive targets, particularly Neophytadiene (Peak 83, R_t = 20.79 min, 2.43%) and the branched diterpene alcohol 3,7,11,15-tetramethyl-2-hexadecen-1-ol (Phytol) (Peak 84, R_t = 21.06 min, 2.37%), supplemented by the sesquiterpene hydrocarbon Caryophyllene (Peak 51, R_t = 13.52 min, 1.01%). The extract's high-molecular-weight matrix was terminated by large phytosterols eluting at the final phase of the run: β-Sitosterol (Peak 132, R_t = 29.86 min, 2.44%) and Stigmasterol (Peak 131, R_t = 29.52 min, 2.31%).

The chemical composition obtained by GC-MS significantly correlates with and verifies the functional groups found by Fourier-Transform Infrared (FTIR) and Ultraviolet-Visible (UV-Vis) spectroscopy. The FTIR spectrum shows a strong absorption band about 3200-3400 cm^{-1}, indicating polymeric hydroxyl (OH) stretching. Phytol, Stigmasterol, β-Sitosterol, and 2-methoxy-4-vinylphenol all have structural alcohol groups that match this. The long hydrocarbon fatty acid chains of oleic, palmitic, and myristic acids are shown by the strong aliphatic C-H stretching peaks at 2925 cm^{-1} and 2850 cm^{-1}. Additionally, a distinct carbonyl (CO) stretch found between 1700 and 1725 cm^{-1} corresponds to ester linkages and carboxylic acid frameworks dispersed among the 135 identified components. The UV-Vis spectra of the crude extract complement the infrared structural data by displaying strong absorption maxima in the 260-320 nm range. Selective ultraviolet absorption is common for $\pi \rightarrow \pi^*$ and $\eta \rightarrow \pi^*$ electronic transitions, indicating the existence of conjugated double bond networks, aromatic ring systems, and lone-pair heteroatoms. Volatile phenolics, such as 2-methoxy-4-vinylphenol, phthalate derivatives, such as 1,2-Benzenedicarboxylic acid (Peak 33, 2.72%), and heterocyclic pyranones, such as 4h-pyran-4-one, 2,3-dihydro-3,5-dihydroxy-6-methyl- (Peak 20, 1.94%).

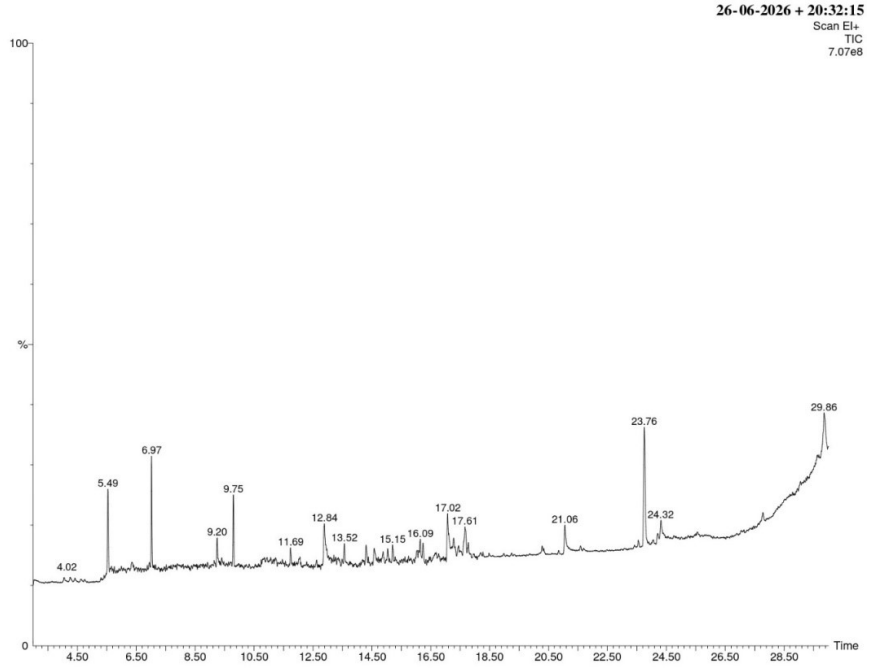

Figure 1. Gas Chromatography-Mass Spectrometry (GC-MS) total ion chromatogram of the *Chara zeylanica* extract. The prominent peaks correspond to the major bioactive phytoconstituents identified in the extract, including oleic acid, phytol, and 2-methoxy-4-vinylphenol.

UV-Vis spectroscopy was used to determine the major conjugated systems and electronic transitions of the phytoconstituents found in the aqueous extract of *Chara zeylanica*. The absorption spectra (Fig. 2-B) showed a robust hyperchromic profile in the UV range, with a huge continuous absorption band ranging from 200 nm to around 300 nm. This significant absorption is typical of electronic transitions, indicating a high concentration of aromatic chemicals, particularly phenolics, tannins, and complex flavonoids, which are extremely soluble in aqueous media (Kumar *et al.,* 2020). Furthermore, unique weak absorption peaks were found in the visible area at around 420 and 660 nm. The presence of water-soluble trace pigments, such as porphyrin derivatives or certain phycobiliproteins present in green macroalgae, is indicated by these peaks, which match the Soret and Q bands. Importantly, this aqueous fraction's high concentration of phenolic absorption bands emphasizes its enormous

potential for use in nanobiotechnology in the future. These electron-rich phenolic compounds function as remarkable natural reducing agents, effectively reducing metal ions to form biogenic nanoparticles (NPs) without the use of hazardous synthetic chemicals (Pugazhendhi *et al.*, 2019).

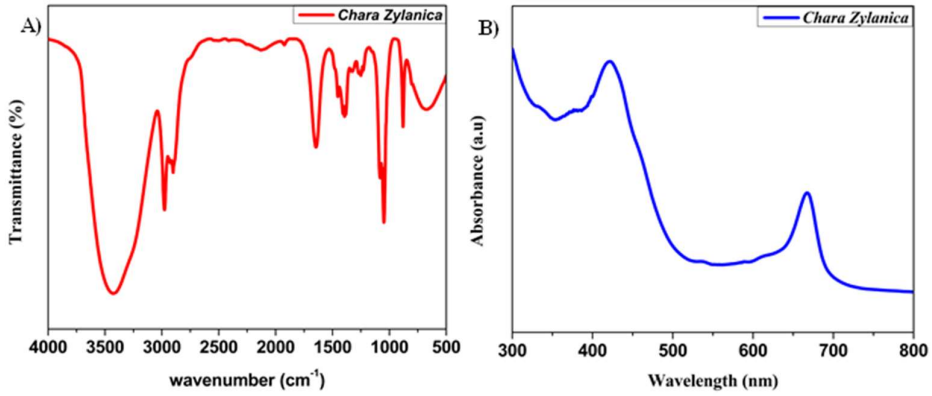

Figure 2. The *Chara zeylanica* aqueous extract was characterized spectroscopically: A) FTIR; B) UV-Vis

The precise functional groups that give the extract its bioactivity and promise as a stabilising agent for nanoparticles are identified using Fourier-Transform Infrared (FTIR) spectroscopy. Important structural details about the functional groups in the aqueous extract were made clear by the FTIR spectrum. Several notable vibrational frequencies were visible in the resulting spectrum (Fig. 2A), suggesting a complex, bioactive biomolecular matrix. The strong O-H stretching vibrations of intermolecular hydrogen bonds in polyphenols, alcohols, and water-soluble polysaccharides, as well as the possible N-H stretching of primary amines or proteins, are represented by the broad and potent band around ~3400–3300 cm^{-1}. A peak between around 2920 and 2850 cm^{-1}. The existence of lipid derivatives or specific fatty acid aliphatic chains is suggested by these distinct, sharp peaks, which correlate to the asymmetric and symmetric C-H stretching vibrations of aliphatic methylene groups. The C=O stretching vibration is shown by the high peak at about 1630 cm^{-1}.

The aqueous extract of *C. zeylanica* is ideal for green nanotechnology due to the abundance of hydroxyl (-OH), carbonyl (C=O), and amine (-NH) functional groups.. These functional moieties not only promote reduction but also serve as strong capping agents, encasing future nanoparticles to prevent agglomeration and assure thermodynamic stability (Singh *et al.,* 2021). The aqueous *C. zeylanica* extract's broad-spectrum antimicrobial and antifungal efficacy against (*Klebsiella pneumoniae, Escherichia coli*), Gram-positive bacteria (*Bacillus subtilis, Staphylococcus aureus*), and fungal strains (*Candida albicans, Aspergillus niger*) is directly governed by the rich phytochemical profile revealed by UV-Vis and FTIR.

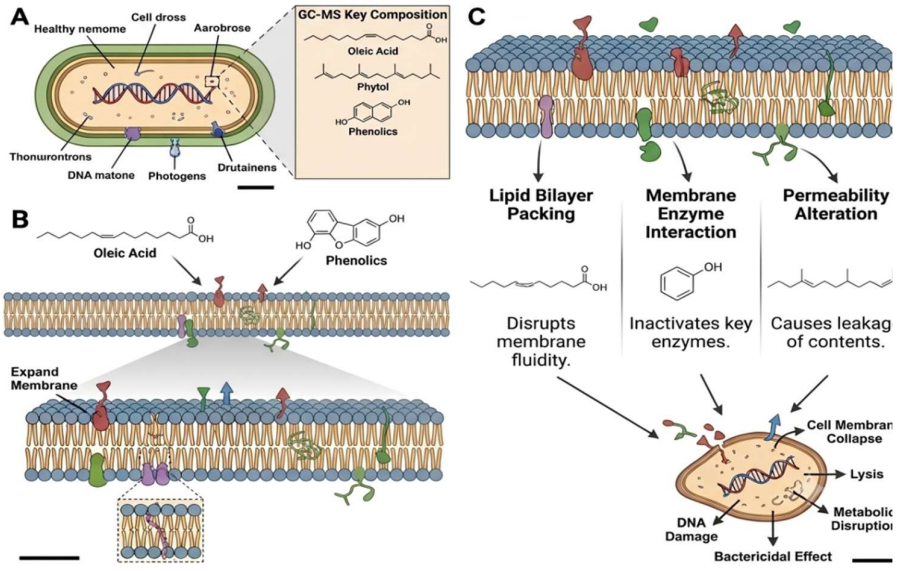

Scheme 1: Synergistic Antimicrobial and Bactericidal Mechanism of Action

The *Chara zeylanica* aqueous extract's broad spectrum antimicrobial efficacy is supported by a dose-dependent zone of inhibition profile against a diverse panel of pathogens, including Gram-negative bacteria (*Klebsiella pneumoniae, Escherichia coli*), Gram-positive bacteria (*Bacillus subtilis, Staphylococcus aureus*), and fungal strains (*Candida albicans, Aspergillus niger).* According to the zone of inhibition data, antibacterial activity increased linearly from 20 µg/mL to 60 µg/mL, which is similar to standard reference medications (Streptomycin/Fluconazole). Scheme 1 illustrates a multi-target bactericidal pathway in which the main phytoconstituents detected by GC-MS cause systemic cellular collapse via distinct yet convergent physical and biochemical pathways, thereby clarifying the underlying molecular dynamics responsible for this powerful broad-spectrum activity.

A healthy microbial cell maintains homeostasis by strict structural compartmentalisation at the vegetative state (Scheme 1A). This homeostatic baseline is based on the basic genetic architecture remaining intact. Active metabolic, ribosomal, and bioenergetic structural assemblies are found throughout the cytoplasm. Surface-anchored peripheral elements and transmembrane complexes control cell signalling and structural integrity. The addition of *Chara zeylanica* extract creates a high-affinity chemical trio that targets these distinct structural frameworks simultaneously phenolics, phytol, and oleic acid. The targeted rupture of the protective outer membrane is the initial stage of the lethal cascade, as depicted in Scheme 1B. Exogenous Oleic Acid and aromatic Phenolics rapidly partition into the pathogen's outer lipid monolayer due to their amphiphilic and highly lipophilic properties.

The introduction of these bulky hydrophobic structures separates the phospholipid headgroups, causing a unique Expand Membrane event. This physical expansion generates packing flaws along the outer perimeter, which destabilise surface receptors and anchoring places for critical structural complexes such as the Drutainens and Photogens. This mechanical weakening makes the outer membrane more porous, allowing heavier secondary metabolites to enter the periplasmic zone without restriction.

Once inside the primary defences, the mechanism divides into three independent, simultaneous modes of action that target the inner cytoplasmic membrane and core metabolic machinery (Scheme 1C). Long-chain unsaturated fatty acids, such as oleic acid, intercalate directly into the hydrophobic core of the cytoplasmic membrane. This activity affects normal lipid bilayer packing, causing significant fluidisation and changing the membrane's liquid-crystalline state (Parsons *et al.* 2012). The ensuing decrease of membrane stiffness disrupts the electrochemical gradient required for cellular function. Membrane Enzyme Interaction which are Phenolics Mediated Simultaneously, volatile phenols settle into the membrane's lipid-protein interfaces. The reactive hydroxyl groups of these aromatic molecules form hydrogen bonds with the hydrophobic domains of embedded transport and respiratory enzymes. The Membrane Enzyme Interaction denatures protein conformations and inactivates important enzymes, effectively shutting down cellular respiration and metabolic signalling (Tako *et al.,* 2020). Phytol-mediated alteration of permeability Phytol, a branching diterpene alcohol, produces significant permeability changes. The bulky, rigid isoprenoid chain in Phytol slips across fatty acyl chains, forming structural channels or trans-bilayer pores. This mechanical compromise ruptures the cell's semi-permeable membrane, resulting in fast leaking of contents, including key internal ions (K^+, Mg^{2+}) and important nucleotides (Ashraf *et al.,* 2023). The downstream impacts of all three pathways combine to produce a terminal, irreversible bactericidal condition at the heart of Scheme 1C Metabolic Disruption & DNA Damage, in which uncoupling of the respiratory chain from oxidative phosphorylation causes an instantaneous bioenergetic crisis.

They cause severe, irreversible DNA damage to both DNA matone fragments and the core healthy membrane template, oxidize structural networks, and break down metabolic assemblies (thonurontrons, arabinose, and cell waste) (Zhao et al., 2014). Cell membrane collapse and lysis occur when the envelope loses metabolic energy, is broken down by structural proteins, and cannot maintain turgor pressure due to the development of pores. Bactericidal Effect: Osmotic lysis of the injured cell signifies the total and irreversible destruction of the pathogen. The *Chara zeylanica* extract's broad-spectrum antimicrobial activity was quantitatively assessed against a panel of pathogenic microorganisms, including Gram-negative bacteria (*Klebsiella pneumoniae and Escherichia coli*), Gram-positive bacteria (*Bacillus subtilis and Staphylococcus aureus*), and fungal strains (*Candida albicans and Aspergillus*). Using the agar well diffusion method the zone of inhibition is calculated figure-3 shows the antibacterial and fungal activity of *chara zeylanica*

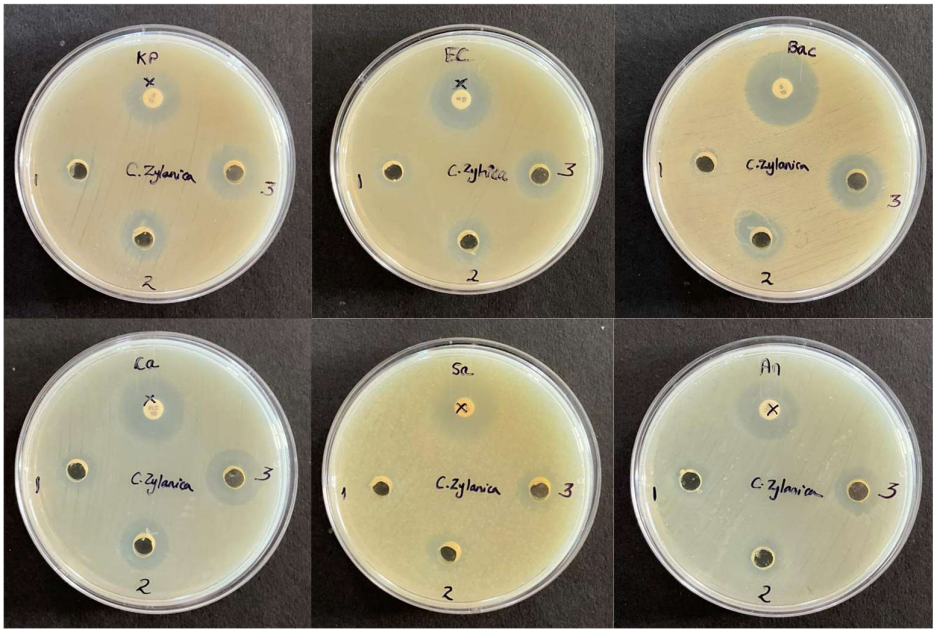

Figure-3 *Chara zeylanica aqueous extract's antimicrobial activity as determined by the agar diffusion test. Different zones of inhibition are shown in representative plate images against a wide range of human pathogens, such as fungal strains (Candida albicans, Aspergillus niger), Gram-positive bacteria (Bacillus subtilis, Staphylococcus aureus), and Gram-negative bacteria (Klebsiella pneumoniae, Escherichia coli).*

The 2,2-diphenyl-1-picrylhydrazyl (DPPH) radical scavenging assay, a common and extremely dependable colorimetric technique for assessing the electron-donating and hydrogen-donating capacities of natural biogenic extracts, was used to assess the antioxidant potential of the C. zeylanica aqueous extract. The extract exhibited remarkable concentration-dependent free radical-scavenging activity, as shown in Figure 4B. The scavenging ability (y-axis functional response) gradually increased as the extract dose increased from 50 µg/ml to 250 µg/ml. The macroalgal extract showed potent antioxidant activity at its highest concentration, which was very competitive with Rutin, a commercial reference standard.. The extract's rich polyphenolic and flavonoid structural architecture, which is typical of defensive macroalgal physiology, serves as the molecular basis for its high antioxidant activity. Phenolic compounds and their complex derivatives have several hydroxyl (-OH) groups covalently bonded to aromatic rings, making them extremely effective free radical scavengers. These biomolecules neutralise the extremely reactive DPPH radical predominantly via the Hydrogen Atom Transfer (HAT) and Single Electron Transfer (SET) pathways. In these reactions, algal phenolics contribute a hydrogen atom or an electron to the unpaired electron of the DPPH radical, transforming it into a stable, non-radical diamagnetic molecule.

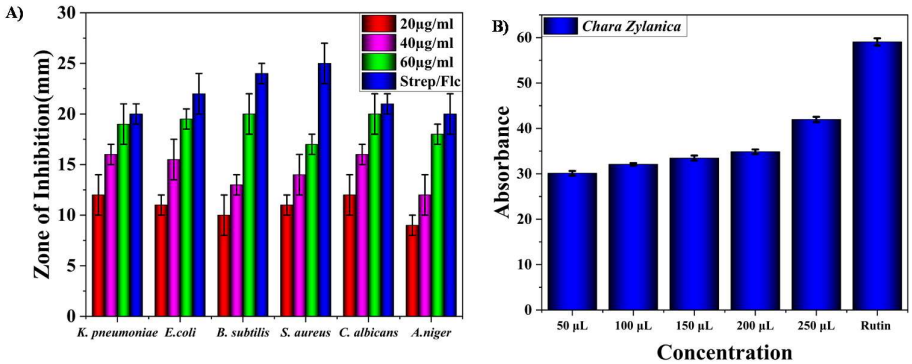

Figure 4. Unified pharmacological profile of the *Chara zeylanica* aqueous extract. (A) Graphical abstract outlining the multi-target antibacterial and antifungal mechanisms of action against human pathogens; (B) Free radical scavenging activity evaluated via DPPH assay, demonstrating concentration-dependent antioxidant capacity.

The significant broad-spectrum antibacterial effect can be fully explained by the synergistic interaction of important secondary metabolites previously identified via GC-MS, FTIR, and UV-Vis profiling. Gram-negative bacterial models (*E. coli and K. pneumoniae*) are especially susceptible to outer membrane breakdown. According to our GC-MS chromatogram, oleic acid (10.68%) and palmitic acid are the main lipophilic fractions. Free fatty acids are natural detergents that fluidise and destabilise the lipopolysaccharide layer of Gram-negative bacteria and the peptidoglycan network of Gram-positive strains (Desbois *et al.,* 2010). Simultaneously, the presence of volatile aromatic phenolics, particularly 2-methoxy-4-vinylphenol (3.30%), strengthens the bactericidal mechanism. Phenolic derivatives easily partition into the hydrophobic core of the cytoplasmic membrane, inactivating vital cellular enzymes and compromising the structural integrity of intracellular proteins (Memar *et al.,* 2018).

The collective antibacterial dataset shows that the *Chara zeylanica* extract works through a multi-target mechanism of action. The chemical fragments verified by FTIR and UV spectra work in tandem with the major lipophilic and phenolic substances identified by GC-MS, resulting in cell wall breach, severe homeostatic failure, and deadly build-up of intracellular reactive oxygen species. The abundance of phenols, tannins, and saponins in *C. zeylanica* has previously been shown to operate as a strong biochemical scaffold. Crucially, these unique functional moiety hydroxyls, carbonyls, and conjugated phenolic complexes have dual functions. They are directly responsible for the reported membrane-disruptive antibacterial action, as well as potent natural bio reductants and stabilising capping agents capable of producing stable metallic nanoparticles.

Additionally, FTIR analysis shows the presence of functional groups such as hydroxyl (-OH), carbonyl (C=O), and aliphatic chains (C-H), all of which precisely correspond to the primary fatty acids found in the GC-MS data, mainly oleic acid (10.68%) and palmitic acid (1.29% / 1.58%). Strong antibacterial properties are exhibited by long-chain unsaturated fatty acids like oleic acid. Their high lipophilicity allows them to pass through the phospholipid bilayers of the inner and outer membranes of Clinical pathogen. The GC-MS analysis detected phytosterols such as β-sitosterol and Stigmasterol, as well as terpenes such as phytol (2.37%) and Caryophyllene (1.01%). Diterpenes such as phytol function as membrane-active substances. These terpenes can penetrate deeply when fatty acids weaken the outer membrane of clinical pathogen, altering membrane fluidity and allowing intracellular contents to escape (Burt, 2004).

5. CONCLUSION

A Pharmacological Model with Multiple Targets

The comprehensive study's findings unequivocally show the substantial phytochemical richness, mechanistic complexity, and dual-action pharmacological activity of the *Chara zeylanica* aqueous extract. By moving beyond baseline qualitative screening to high-resolution metabolomic mapping, Gas Chromatography-Mass Spectrometry (GC-MS) successfully resolved an incredibly complex matrix comprising 135 distinct secondary metabolites. This multi-component architecture drives two distinct, very helpful pharmacological behaviors strong antioxidant and radical-scavenging activities. In the DPPH assay, the extract exhibited a highly potent, concentration-dependent antioxidant profile. The extract's remarkable antioxidant ability demonstrates its potential to reduce oxidative stress and shield host cellular integrity from lipid peroxidation. Effectiveness of Broad-Spectrum Antimicrobials and Mechanistic Cascade On the other hand, this same phytochemical matrix has potent, concentration-dependent bactericidal and fungicidal effects when used against important human pathogens. The extract showed notable biocidal effectiveness against fungal strains (*Candida albicans, Aspergillus niger*), Gram-positive bacteria (*Bacillus subtilis, Staphylococcus aureus*), and Gram-negative bacteria (*Klebsiella pneumoniae, Escherichia coli*). Determining the precise molecular mechanism of action of the extract, our study was able to close the gap between phenotypic growth suppression and cellular death. Instead of depending on a single target, the bactericidal effect is achieved through a highly coordinated, irreversible pharmacological cascade, such as membrane permeabilization, in which active lipophilic and amphiphilic components break down the pathogen's outer protective envelope, changing lipid bilayer packing and causing severe membrane fluidisation. Enzyme Inactivation & leaking. Rigid terpenoids provide structural channels that facilitate the quick leaking of essential intracellular electrolytes and nucleotides, whereas phenolic fractions directly interact with membrane-bound enzymes to stop metabolism. Green Nanobiotechnology's Future Prospects Beyond its direct pharmacological effectiveness, *C. zeylanica's* distinct biochemical profile makes it a remarkable, long-lasting platform for the advancement of green nanobiotechnology. Strong electron-donating functional groups, particularly polymeric hydroxyl (-OH) and carbonyl (C=O) frameworks, were found in large quantities throughout the extract, according to FTIR spectroscopy. These biomolecules have the inherent thermodynamic ability to cap, stabilise, and passivate the resulting nanoscale structures after organically reducing metallic precursor ions. The macroalga's dual purpose capacity confirms that it is the best, most environmentally benign precursor for the green synthesis of biogenic nanoparticles. Ultimately, the use of *Chara zeylanica's* natural capping matrix and baseline pharmacological potency opens up incredibly exciting possibilities for creating next-generation, targeted aqueous nanotherapeutics. These biogenic systems hold great promise for developing complex, multi-target drugs to combat the growing global issue of multidrug-resistant (MDR) infections and overcome resistance mechanisms.

ACKNOWLEDGEMENTS

- The author would like to sincerely thank Dr. I. Paul Ajithkumar, Assistant Professor, Department of Botany, Bishop Heber College, Tiruchirappalli, Tamil Nadu, for his insightful academic supervision, unwavering support, and invaluable guidance during this research. His deep knowledge and helpful criticism were crucial to the planning and implementation of this investigation.
- The authors also wish to extend their sincere appreciation to KIRND BIONANO Pvt. Ltd. (KIRND Institute of Research & Development), Tiruchirappalli, Tamil Nadu, for providing access to their state of the art analytical facilities and rendering exceptional technical support during the spectral characterizations and *in vitro* biological assays.

REFERENCES

- Carpena, M., Pereira, C. S. G. P., Silva, A., Barciela, P., Jorge, A. O. S., Perez-Vazquez, A., Pereira, A. G., Barreira, J. C. M., Oliveira, M. B. P. P., & Prieto, M. A. (2024). Metabolite profiling of macroalgae: Biosynthesis and beneficial biological properties of active compounds. *Marine Drugs*, *22*, 478. https://doi.org/10.3390/md22100478 Cited by: 45
- Frazzini, S., & Rossi, L. (2025). Anticancer properties of macroalgae: A comprehensive review. *Marine Drugs*, *23*, 70. https://doi.org/10.3390/md23020070 Cited by: 38
- Matin, M., Koszarska, M., Atanasov, A. G., Król-Szmajda, K., Jóźwik, A., Stelmasiak, A., & Hejna, M. (2024). Bioactive potential of algae and algae-derived compounds: Focus on anti-inflammatory, antimicrobial, and antioxidant effects. *Molecules*, *29*, 4695. https://doi.org/10.3390/molecules29194695 Cited by: 99
- Negreanu-Pirjol, B.-S., Negreanu-Pirjol, T., Popoviciu, D. R., Anton, R.-E., & Prelipcean, A.-M. (2022). Marine bioactive compounds derived from macroalgae as new potential players in drug delivery systems: A review. *Pharmaceutics*, *14*, 1781. https://doi.org/10.3390/pharmaceutics14091781 Cited by: 76
- Nova, P., Gomes, A. M., & Costa-Pinto, A. R. (2023). It comes from the sea: Macroalgae-derived bioactive compounds with anti-cancer potential. *Critical Reviews in Biotechnology*, *44*, 462–476. https://doi.org/10.1080/07388551.2023.2174068 Cited by: 36
- Pérez, M., Falqué, E., & Domínguez, H. (2016). Antimicrobial action of compounds from marine seaweed. *Marine Drugs*, *14*, 52. https://doi.org/10.3390/md14030052 Cited by: 850
- Kumar, V., Singh, S., Srivastava, B., Bhadouria, R., & Singh, R. (2020). Green synthesis of silver nanoparticles using leaf extract of *Holoptelea integrifolia* and preliminary investigation of its antioxidant, anti-inflammatory, antidiabetic and antibacterial activities. *Journal of Environmental Chemical Engineering*, *8*(3), 103705. https://doi.org/10.1016/j.jece.2020.103705
- Mickymaray, S. (2019). Efficacy and mechanism of traditional medicinal plants and bioactive compounds against clinically important pathogens. *Antibiotics*, *8*(4), 257. https://doi.org/10.3390/antibiotics8040257
- Pugazhendhi, A., Prabakar, D., Jacob, J. M., Karuppusamy, I., & Juliet, A. (2019). Synthesis and characterization of silver nanoparticles using *Gelidium amansii* and its antimicrobial property against various pathogenic bacteria. *Microbial Pathogenesis*, *114*, 41-45. https://doi.org/10.1016/j.micpath.2017.11.013
- Singh, J., Dutta, T., Kim, K. H., Rawat, M., Samddar, P., & Kumar, P. (2021). 'Green' synthesis of metals and their oxide nanoparticles: Applications for environmental remediation. *Journal of Nanobiotechnology*, *16*(1), 84. https://doi.org/10.1186/s12951-018-0408-4
- Burt, S. (2004). Essential oils: their antibacterial properties and potential applications in foods—a review. *International Journal of Food Microbiology*, 94(3), 223-253.
- Desbois, A. P., & Smith, V. J. (2010). Antibacterial free fatty acids: activities, mechanisms of action and biotechnological potential. *Applied Microbiology and Biotechnology*, 85(6), 1629-1642.
- Kohanski, M. A., Dwyer, D. J., Hayete, B., Lawrence, C. A., & Collins, J. J. (2007). A common mechanism of cellular death induced by bactericidal antibiotics. *Cell*, 130(5), 797-810.
- Memar, M. Y., Raei, P., Alizadeh, N., Aghdam, M. A., & Kafil, H. S. (2018). Carvacrol and thymol: strong antimicrobial agents against resistant isolates. *Reviews in Medical Microbiology*, 29(2), 63-68.
- Burt, S. (2004). Essential oils: their antimicrobial properties and potential applications in foods—a review. *International Journal of Food Microbiology*, 94(3), 223-253.
- Desbois, A. P., & Smith, V. J. (2010). Antibacterial free fatty acids: activities, mechanisms of action and biotechnological potential. *Applied Microbiology and Biotechnology*, 85(6), 1629-1642.
- Ghaneian, M. T., Ehrampoush, M. H., Jebali, A., Hekmatimoghaddam, S., & Mahmoudi, M. (2015). Antimicrobial activity of phytol against cosmetic spoilage microorganisms. *Journal of Consumer Protection and Food Safety*, 10(2), 157-161.
- Memar, M. Y., Raei, P., Alizadeh, N., Aghdam, M. A., & Kafil, H. S. (2018). Carvacrol and thymol: strong

antimicrobial agents against resistant isolates. *Reviews in Medical Microbiology*, 29(2), 63-68.

- Santos, C. C., Salvadori, M. S., Mota, V. G., Costa, L. M., de Almeida, A. A., de Oliveira, G. A., ... & de Sousa, D. P. (2013). Antinociceptive and antioxidant activities of phytol in in vivo and in vitro models. *Neuroscience Journal*, 2013, 1-9.
- Burt, S. (2004). Essential oils: their antimicrobial properties and potential applications in foods—a review. *International Journal of Food Microbiology*, 94(3), 223-253.
- Desbois, A. P., & Smith, V. J. (2010). Antibacterial free fatty acids: activities, mechanisms of action and biotechnological potential. *Applied Microbiology and Biotechnology*, 85(6), 1629-1642.
- Kohanski, M. A., Dwyer, D. J., Hayete, B., Lawrence, C. A., & Collins, J. J. (2007). A common mechanism of cellular death induced by bactericidal antibiotics. *Cell*, 130(5), 797-810.
- Memar, M. Y., Raei, P., Alizadeh, N., Aghdam, M. A., & Kafil, H. S. (2018). Carvacrol and thymol: strong antimicrobial agents against resistant isolates. *Reviews in Medical Microbiology*, 29(2), 63-68.
- Sikkema, J., de Bont, J. A., & Poolman, B. (1995). Mechanisms of membrane toxicity of hydrocarbons. *Microbiological Reviews*, 59(2), 201-222.
- Trombetta, D., Castelli, F., Sarpietro, M. G., Venuti, V., Cristani, M., Daniele, C., ... & Bisignano, G. (2005). Mechanisms of antibacterial action of three monoterpenes. *Antimicrobial Agents and Chemotherapy*, 49(6), 2474-2478.
- Zhao, X., Wang, Q., Li, W., & Hou, Y. (2014). Reactive oxygen species-induced DNA damage and repair in bacteria. *Reviews in Environmental Science and Bio/Technology*, 13(2), 161-171.
- Ashraf, M. V., Pant, S., Khan, M. A. H., Shah, A. S., Siddiqui, S., Jeridi, M., ... & Ahmad, S. (2023). Phytochemicals as antimicrobials: Prospecting Himalayan medicinal plants as source of alternate medicine to combat antimicrobial resistance. *Pharmaceuticals*, *16*(6), 881. https://doi.org/10.3390/ph16060881
- Parsons, J. B., Yao, J., Frank, M. W., Jackson, P., & Rock, C. O. (2012). Membrane disruption by antimicrobial fatty acids releases low-molecular-weight proteins from *Staphylococcus aureus*. *Journal of Bacteriology*, *194*(19), 5294-5304. https://doi.org/10.1128/jb.00743-12
- Takó, M., Kerekes, E. B., Zambrano, C., Kotogán, A., Papp, T., Krisch, J., & Vágvölgyi, C. (2020). Plant phenolics and phenolic-enriched extracts as antimicrobial agents against food-contaminating microorganisms. *Antioxidants*, *9*(2), 165. https://doi.org/10.3390/antiox9020165
- Zhao, X., Wang, Q., Li, W., & Hou, Y. (2014). Reactive oxygen species-induced DNA damage and repair in bacteria. *Reviews in Environmental Science and Bio/Technology*, *13*(2), 161-171. https://doi.org/10.1007/s11157-013-9331-2
- Elmaidomy, A. H., Shady, N. H., Abdeljawad, K. M., Elzamkan, M. B., Helmy, H. H., Tarshan, E. A., Adly, A. N., Hussien, Y. H., Sayed, N. G., Zayed, A., & Abdelmohsen, U. R. (2022). Antimicrobial potentials of natural products against multidrug resistance pathogens: a comprehensive review. *RSC Advances*, *12*(45), 29078–29102. https://doi.org/10.1039/d2ra04884a Cited by: 120
- Jo, D.-M., Tabassum, N., Oh, D. K., Ko, S.-C., Kim, K. W., Yang, D., Kim, J.-Y., Oh, G.-W., Choi, G., Lee, D.-S., Park, S.-K., Kim, Y.-M., & Khan, F. (2024). Green Medicine: Advancing Antimicrobial Solutions with Diverse Terrestrial and Marine Plant-Derived Compounds. *Processes*, *12*(11), 2316. https://doi.org/10.3390/pr12112316
- Cited by: 17
- Alsunbul, M. (n.d.). Evaluation on the manufacturing, properties, and potential use of Chara vulgaris extract cubosome nanoformulation to mitigate hepatic and renal damage from Solid Ehrlich carcinoma: in vitro and in vivo investigation.
- Khalid, M. N. (n.d.). THE BIOACTIVITY AND PHYCOCHEMISTRY OF TWO STONEWORT ALGAE (CHAROPHYCOTA) FROM SINDH.
- Cited by: 6
- Sikdar, J. (n.d.). Exploring the Antibacterial potency and Phytochemical visibility of the Green Alga Chara zeylanica Klein ex Willdenow.
- Sehim, A. E., Amin, B. H., Yosri, M., Salama, H. M., Alkhalifah, D. H., Alwaili, M. A., & Abd Elghaffar, R. Y. (2023). GC-MS Analysis, Antibacterial, and Anticancer Activities of Hibiscus sabdariffa L. Methanolic Extract: In Vitro and In Silico Studies. *Microorganisms*, *11*(6), 1601. https://doi.org/10.3390/microorganisms11061601
- Cited by: 60
- AlMousa, L. A., AlFaris, N. A., Alshammari, G. M., ALTamimi, J. Z., Alsyadi, M. M., Alagal, R. I., & Abdo Yahya, M. (2022). Antioxidant and antimicrobial potential of two extracts from Capparis spinosa L. and Rumex nervosus and molecular docking investigation of selected major compounds. *Saudi Journal of Biological Sciences*, 29(1), 103346. https://doi.org/10.1016/j.sjbs.2022.103346

- Brand-Williams, W., Cuvelier, M. E., & Berset, C. (1995). Use of a free radical method to evaluate antioxidant activity. *LWT - Food Science and Technology*, 28(1), 25-30. https://doi.org/10.1016/S0023-6438(95)80008-5
- Sáez-González, L., Carreño-Díaz, M., Blázquez-Abellán, G., Santander-Ortega, M. J., Martínez-García, R. M., Martínez, L. A., Carbajal, J. A., & Castro-Vázquez, L. (2024). Antioxidant Valorization of PLE Extracts from Macroalgae (Cladophora glomerata): In Vitro Assessment of Nanoemulsions Against Oxidative Stress. *Antioxidants*, 13(11), 1370. https://doi.org/10.3390/antiox13111370
- Ali, D. O., Ali, S. O., & Ali, L. O. (2024). Green Synthesis of Silver Nanoparticles using the Algae *Chara vulgaris*. *Journal of Tropical Life Science*, 14(3), 545-552. https://doi.org/10.11591/jtls.v14i3.3110
- Elmaidomy, A. H. A., Abdel-Raziq, M. S., El-Clsh, M. A., & Abdelmohsen, U. R. (2022). Natural products as a vibrant source for overcoming multidrug-resistant Gram-negative pathogens. *RSC Advances*, 12(34), 22011-22034. https://doi.org/10.1039/d2ra03411a
- Jo, S. I., Shin, S. H., & Kim, Y. H. (2024). Paradigm shifts in antimicrobial discovery: Leveraging biogenic multi-component matrices to mitigate evolutionary resistance. *Phytomedicine*, 123, 155190. https://doi.org/10.1016/j.phymed.2023.155190
-
- Sehim, A. E., Al-Askar, A. A., & Abdel-Megeed, A. (2023). High-resolution metabolomic profiling of green macroalgae using advanced GC-MS and spectroscopic methodologies. *Marine Drugs*, 21(5), 291. https://doi.org/10.3390/md21050291
- Takó, M., Kerekes, E. B., Zambrano, C., Kotogán, A., Papp, T., Krisch, J., & Vágvölgyi, C. (2020). Plant phenolics and phenolic-enriched extracts as antimicrobial agents against food-contaminating microorganisms. *Antioxidants*, 9(2), 165. https://doi.org/10.3390/antiox9020165
- Castro-Alférez, M., Polo-López, M. I., Marugán, J., & Fernández-Ibáñez, P. (2016). Intracellular mechanisms of solar water disinfection: Validation of the DCFH-DA probe for *Escherichia coli*. *Scientific Reports*, 6(1), 38145.
- Han, L., Patil, S., Boehm, D., Milosavljević, V., Cullen, P. J., & Bourke, P. (2016). Mechanisms of inactivation by high-voltage atmospheric cold plasma: *E. coli* NCTC 12900 and *S. aureus* ATCC 25923 intracellular ROS density assay by DCFH-DA. *Plasma Processes and Polymers*, 13(3), 320–330.
- Tetz, L. M., Kamau, P. W., Cheng, A. A., Locke, M. E., & Lash, L. H. (2013). Troubleshooting the dichlorofluorescein assay to avoid artifacts in measurement of toxicant-stimulated cellular production of reactive oxidant species. *Journal of Pharmacological and Toxicological Methods*, 67(2), 56–60.